CHAPTER 191

Even/Odd Analysis of Shoreline Changes Adjacent to Florida's Tidal Inlets

Paul A. Work¹ and Robert G. Dean²

Abstract

Measured shoreline changes up— and downdrift of several tidal inlets on the eastern coast of Florida are decomposed into even and odd components. The odd component of shoreline change is compared to both analytical and numerical predictions of shoreline response to a shore–normal littoral barrier. A best–fit iterative scheme is used for application of the analytical solution. The numerical solution improves upon the analytical approach by accounting for refraction, diffraction, and wave energy dissipation on the ebb tidal shoal. Predicted and measured changes agree reasonably well for several cases, and future refinements and improved long–term wave data are expected to allow more accurate prediction of smaller–scale features.

Introduction

Formation of a tidal inlet, whether resulting from natural events or human activity, often leads to large-scale, long-term shoreline changes, as the inlet represents an interruption of longshore sediment transport. This is particularly true where the inlet is stabilized by training structures, as is common along the eastern coast of Florida. The wave climate that provides the energy to mobilize the sediment is in turn altered by the evolving beach-inlet system. The resulting situation is often a complex wave field where wave breaking, diffraction, and refraction due to both tidal currents and time-varying bathymetry are all important.

A shore–normal littoral barrier placed along a coast having a strongly dominant direction associated with its longshore sediment transport will typically lead to the familiar result of accretion updrift and erosion downdrift of the barrier. In the field, other processes often complicate the picture. For this reason, a method is presented by which the "shoreline signature" of an inlet may be decomposed for study. The method has been applied to a number of tidal inlets along Florida's eastern coast, and analytical and numerical simulations of shoreline change have been generated for comparison. Figure 1 shows the locations of the tidal inlets addressed in this paper.

 $^{^1}$ Graduate Research Assistant, Coastal and Oceanographic Engineering, University of Florida, Gainesville, Florida 32611 USA

²Graduate Research Professor, Coastal and Oceanographic Engineering, University of Florida, Gainesville, Florida 32611 USA



Figure 1: Locations of tidal inlets studied.

Several goals of the study were defined: to investigate and interpret shoreline changes at tidal inlets, examine the effectiveness of methods for prediction of these changes, and suggest improvements to these methods. The focus throughout the study was on changes directly attributable to the presence of the inlet.

Analytical Solution

A method by which shoreline response to a shore–normal littoral barrier may be predicted was proposed by Pelnard–Considère (1956). It is assumed that all offshore contours behave similarly, reducing the problem to the description of the position of one contour, typically the shoreline (hence the term "one–line model"). The x-axis is placed along the shoreline and the y-axis directed offshore. The coordinate system origin is at the point where the initial shoreline and the littoral barrier intersect.

Assuming that the wave crests are nearly shore–parallel, a sediment continuity equation may be combined with a dynamic sediment transport equation and linearized to show that the problem is governed by the heat, or diffusion equation (Pelnard–Considère, 1956):

$$\frac{\partial y}{\partial t} = G \frac{\partial^2 y}{\partial x^2} \tag{1}$$

where G is a diffusivity parameter containing, most importantly, the breaking wave height:

$$G = \frac{KH_b^{5/2}\sqrt{g/\kappa}}{8(s-1)(1-p)(h_* + B)}$$
 (2)

where

K = Dimensionless transport coefficient of order 1

 $H_b = \text{Wave height at breaking}$

g = Acceleration of gravity

 $\kappa = H_b/h_b$ (Spilling breaker assumption)

 h_b = Water depth at breaking s = Sediment specific gravity

p = Sediment porosity

 $h_* = \text{Maximum depth of sediment motion, or depth of closure } B = \text{Berm height}$

Note that G has units of length squared per unit time.

A solution to Equation 1 requires application of appropriate boundary conditions, and an initial condition:

$$y(\pm \infty, t) = 0$$
, for all t (3)

$$y(x,0) = 0, \quad |x| < \infty \tag{4}$$

specifying no change in the far-field and a shoreline that is initially straight. The boundary condition at the barrier consists of two parts, the second part being invoked subsequent to the initiation of sediment bypassing around the tip of the littoral barrier:

$$\frac{\partial y}{\partial x}\Big|_{x=0} = \tan \theta_b \quad 0 < t < t_{bp} \tag{5}$$

$$y(0,t) = \pm l \qquad t \ge t_{bp} \tag{6}$$

where θ_b is the angle (measured counter-clockwise) between the shore-normal and the wave ray at breaking, and l denotes the length of the littoral barrier. The positive sign in Equation 6 corresponds to the updrift side of the barrier. The first part of this boundary condition forces the shoreline at the structure to parallel the wave crests, resulting in zero longshore transport past the structure. The second part (which is approximate) fixes the shoreline to the end of the barrier.

The time of bypassing, t_{bp} , may be expressed in terms of known quantities:

$$t_{bp} = \frac{\pi}{G} \frac{l^2}{4 \tan^2 \theta_b} \tag{7}$$

The solution to this problem is given by Equations 8 and 9. The solution is presented here only for x > 0, but it is noted that the solution is anti-symmetric about the y-axis, i.e. y(-x,t) = -y(x,t).

$$y(x,t) = \frac{-\tan\theta_b}{\sqrt{\pi}} \left[\sqrt{4Gt} \exp\left(-\frac{x^2}{4Gt}\right) - x\sqrt{\pi} \operatorname{erfc}\left(\frac{x}{\sqrt{4Gt}}\right) \right] \quad \text{for } t < t_{bp} \quad (8)$$

and

$$y(x,t) = -\frac{\tan \theta_b}{|\tan \theta_b|} l\operatorname{erfc}\left(\frac{x}{\sqrt{4Gt}}\right) \quad \text{for } t \ge t_{bp}$$
 (9)

where erfc denotes the complimentary error function. The solution given by Equations 8 and 9 will be applied for the prediction of shoreline changes at a tidal inlet by assuming that the inlet itself has negligible width. Several additional assumptions have been invoked to achieve this result: the littoral barrier is assumed impermeable, the shoreline is homogeneous, and the wave climate does not vary in the x-direction or in time. Also note that sediment is conserved; all sediment bypassing the structure reaches the downdrift shore. These assumptions are not well–suited to all field sites, suggesting that attempts be made to relax some of them. One approach is described below.

Even/Odd Decomposition of Measured Shoreline Changes

At this point it is appropriate to consider the measured shoreline changes to which predictions will be compared. Digitized historical charts and surveys were obtained from the Department of Natural Resources, State of Florida (Foster and Savage, 1989; Savage and Foster, 1989). Using the coordinate system of the previous section, surveys from different dates were compared to determine a net shoreline change "function", $y_N(x)$. An attempt was made to select a first survey corresponding to the time at which the inlet was constructed or stabilized. The second (later) survey was chosen to place it before any beach nourishment or sand bypassing projects, but long enough after inlet construction that long-term shoreline changes dominated over seasonal changes.

It was decided to divide the shoreline change function, $y_N(x)$, into even (symmetric about the y-axis) and odd (anti-symmetric) components. This can be done easily for any function, with the two components given as follows (Berek and Dean, 1982; Dean and Pope, 1987):

$$y_E(x) = \frac{y_N(x) + y_N(-x)}{2} \tag{10}$$

$$y_O(x) = \frac{y_N(x) - y_N(-x)}{2} \tag{11}$$

The justification for this approach becomes evident when one considers the contributions to shoreline change at a tidal inlet. The interruption of longshore sediment transport should, according to the analytical solution of the previous section, contribute only an odd component. Storms and sea level rise will tend to exert similar influences on both sides of the domain, leading to an even component. Refraction and diffraction effects will vary, possibly contributing to both even and odd components.

It can easily be demonstrated that sand bypassing will add a "negative" odd component; i.e. an odd component that reduces the offset created by the presence of a littoral barrier, and that beach nourishment will tend to contribute to both even and odd components. The effects of factors leading to the presence of an even component are often difficult to predict, and most would exist even without the presence of the inlet. The primary influence of the inlet is a blockage of longshore sediment transport, so it was decided to compare predicted shoreline

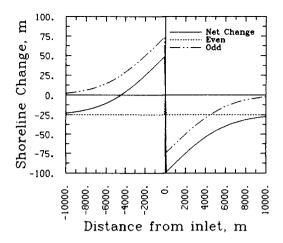


Figure 2: Analytical solution with superimposed uniform background erosion of 25 m in 75 years. l=75 m, $H_b=0.5$ m, and $\theta_b=1^{\circ}$. All shoreline change plots are oriented to place the ocean at top.

changes to the odd component of measured shoreline changes.

A simple, illustrative example is helpful. If a uniform background erosion is superimposed upon the analytical solution of the previous section, the result shown in Figure 2 is obtained. Note that for this case, decomposition into even and odd components simply returns the initial constituents, since the analytical solution is odd and the background erosion even. Also note that any loss or gain of sediment within the domain is revealed by the integral of the even component, as the integral of the odd component is zero.

Best-Fit Analytical Solution

Application of the analytical solution requires confident estimates of several parameters, including wave height and direction at breaking, and the length of the jetty. The jetty length may seem to be well known, but three factors complicate selection of a value for this parameter: structure permeability, physical modifications which take place during the time period of interest, and the fact that portions of the active, updrift profile extend beyond the jetty tip well before the shoreline reaches the jetty tip. These factors suggest the use of an "effective" jetty length. Lacking long-term values for the parameters, a best-fit technique was developed to compare the analytical solution to the odd component of measured shoreline change.

An iterative scheme was developed to find parameters that minimized the mean square difference, or error, between the analytical solution and the odd component of measured shoreline change. This error is defined as follows:

$$\varepsilon^2 = \frac{1}{N} \sum_{i=1}^{N} \left[y_A(x_i, t) - y_O(x_i) \right]^2 \tag{12}$$

where x_i denotes the longshore coordinate of the *i*th point, $y_O(x_i)$ the value of the odd component at that point, $y_A(x_i,t)$ the analytical solution, and N the number of data points available.

The best fit will exist when the derivative of ε^2 with respect to each parameter is zero. Initially, only the pre-bypassing portion of the analytical solution, which has no dependence on jetty length, was used. The two parameters allowed to vary were the diffusivity, G (containing the wave height at breaking), and the tangent of the wave angle at breaking, $\tan \theta_b$. Figure 3 gives contours of equal values of ε , plotted against G and $\tan \theta_b$, for Ft. Pierce Inlet. This inlet was constructed in 1921, but the first of the two surveys used to determine the odd component of shoreline change is from 1928. For cases such as this, the analytical solution used in the best-fit procedure is defined as the difference between the solution at the time of the second survey $(t_{end}, 46$ years for this case) and the solution at the time of the first survey $(t_{start}, 7$ years here). All times are thus referenced to the construction of the inlet.

The best-fit methodology was then extended to include both parts of the analytical solution (pre- and post-bypassing) and thus allow for the variation of jetty length, l. This then accomodates three scenarios, depending on whether the surveys are dated before or after initiation of bypassing. Note that if both surveys are pre-bypassing, jetty length cannot be inferred, since the pre-bypassing solution has no dependence on jetty length. Similarly, if both surveys are post-bypassing, wave direction is indeterminable. Only if the first survey is pre-bypassing and the ending survey post-bypassing can wave height, direction, and jetty length all be determined. This last scenario occurred for only one case, that of Ft. Pierce Inlet. For each of the other cases, the pre-bypassing solution provided the best fit. Figure 4 compares the measured odd component for Ft. Pierce Inlet to the two best-fit solutions; Figure 5 illustrates the error surface when the full analytical solution is allowed. This error surface depends on three variables, and is therefore four-dimensional. The jetty length has been "frozen" at its best-fit value for illustration. Note that the full solution for this case provides a very good fit, but the associated wave angle (8.4 degrees) appears unreasonably large for a long-term average.

The error surface that results when the full analytical solution is used (Figure 5) should have at least three relative minima: one corresponding to the case where both surveys predate bypassing; one where the surveys lie to either side of the time of bypassing; and one where both surveys post-date initiation of bypassing. Recall that the time of bypassing depends on G, $\tan \theta_b$, and l, so varying any of these parameters changes the time of bypassing. One could allow any number of the available parameters to vary, but it was felt that the three chosen contained the most uncertainty.

Numerical Model

A numerical model was developed to investigate the effects of wave refraction due to both bathymetry and tidal currents, diffraction of energy into the "shadow zone" in the lee of the downdrift jetty, and the sheltering effect of an ebb tidal

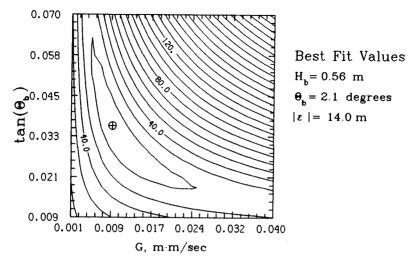


Figure 3: Contours of equal error, $|\varepsilon|$, for Ft. Pierce Inlet, 1928–1967. Prebypassing solution only.

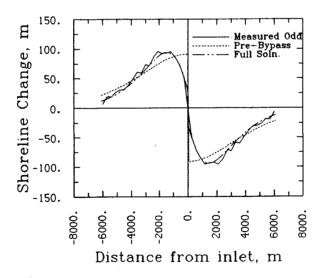


Figure 4: Measured odd component and the two best-fit solutions for Ft. Pierce Inlet, 1928–1967.

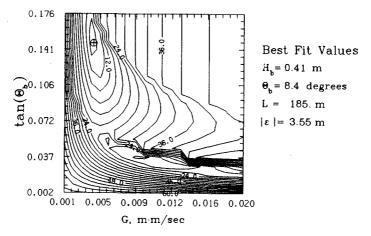


Figure 5: Error surface for Ft. Pierce Inlet, 1928–1967. Full analytical solution.

shoal.

The model includes a two-dimensional finite-difference wave propagation routine, providing the nearshore wave climate for computation of shoreline change by a one-line finite-difference model. The primary advantage of this method over the analytical solution is that spatial and temporal variability in the nearshore wave climate can be accommodated. The governing equation and boundary conditions for the sediment model remain unchanged.

Wave conditions at the offshore boundary are specified and the bathymetry and tidal currents approximated analytically. The dispersion relationship including the effects of currents is given in terms of an intrinsic wave frequency, σ :

$$\sigma^2 = gk \tanh kh \tag{13}$$

where

$$\sigma = \omega - \vec{k} \cdot \vec{u}$$

$$\omega = \text{absolute frequency} = 2\pi/T$$

$$T = \text{wave period}$$

$$\vec{u} = \text{mean current vector}$$

$$\vec{k} = \text{wavenumber vector}$$

$$h = \text{water depth}$$

Irrotationality of the wavenumber vector specifies wave direction:

$$\nabla \times \vec{k} = 0 \tag{14}$$

and conservation of wave action is applied to solve for wave height:

$$\nabla \cdot \left[\frac{E}{\sigma} \left(\vec{u} + \vec{C}_g \right) \right] = 0 \tag{15}$$

where

 $E = \text{Wave energy density} = \rho g H^2/8$ $\vec{C}_g = \text{wave group velocity vector}$

Starting at the offshore boundary, Equations 13, 14, and 15 were applied iteratively at each grid point to solve for wavenumber vector, \vec{k} , and wave height, H. To account for wave energy dissipation across a shoal or other bathymetric feature, the wave height was checked at each point and truncated to 78% of the water depth if it exceeded this height. Diffraction of wave energy into the sheltered area behind the jetty was included through application of the method of Perlin and Dean (1985).

The best-fit analytical solution was used to determine the offshore wave climate for the numerical model. The best-fit wave direction and height were transformed offshore using Snell's Law and conservation of wave energy flux. For each inlet studied, the analytical and numerical predictions of shoreline change differ little. The primary factor accounting for this is that the wave climate used as input to the numerical model represents a long-term average, with a relatively small wave height, and the direction deviates little from shore-normal. Thus wave energy dissipation on the shoal (where one is present) and wave diffraction are thought to be under-predicted in the numerical model.

Sensitivity tests indicate that moderate tidal currents have little effect on the results. This appears reasonable, since the modelled domain typically extends up to 10 km to either side of the inlet, well outside the zone of strong tidal influence.

Results

Shoreline changes at each of the tidal inlets along the eastern coast of Florida for which data were available were studied by the techniques described above. As might be expected, the analytical and numerical predictive methods appear to be best suited to inlets that are stabilized at the time of construction by relatively impermeable jetty structures.

Figure 6 shows the odd component of measured shoreline change, the best-fit analytical solution, and the numerical simulation for Ft. Pierce Inlet. The pre-bypassing best-fit solution is used here, as the full solution yielded unreasonable wave parameters. Agreement is fairly good except near the inlet, suggesting for this case that the initial accretion/erosion immediately adjacent to the inlet is underestimated. Reversals in the direction of longshore sediment transport could also contribute to this feature. Note that the predictions do not include any of the small-scale deviations seen in the measured odd component. The models tend to smooth out any irregularities in the shoreline, given sufficient time.

Results for St. Lucie Inlet, which was constructed in 1892, are presented in Figure 7. The inlet was initially stabilized only on its north side, the south jetty being added in 1982. The shape of the solutions match the measured odd component well, despite the fact that several of the assumptions implicit in the solutions (impermeable structures on both sides of the inlet, homogeneous shoreline, no temporal variation in wave climate) are not well–satisfied at this inlet. As with each of the inlets discussed here, the net longshore transport of sediment is directed to the south, but reversals are common in the summer season.

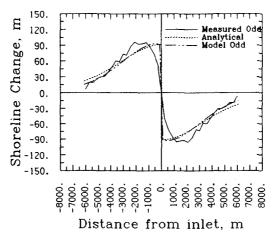


Figure 6: Measured odd component and predictions of shoreline change for Ft. Pierce Inlet, 1928–1967 (inlet constructed 1921). $H_b = 0.56 \text{ m}$, $\theta_b = 2.1 \text{ degrees}$.

Figure 8 presents results for Sebastian Inlet. This inlet was constructed in 1924, but closed naturally in 1941–42. It was then re-opened in 1948 and has remained open to date. The results shown in Figure 8 neglect the closure of the inlet from 1942–1948. The magnitude of the shoreline change for this case is smaller, so small-scale deviations from the predicted changes are more evident.

Figure 9 provides results for Port Canaveral, constructed in 1951. Agreement between the measured and predicted changes is not as good here, and it is seen that there is a spike in the measured odd component for $x=\pm 4000$ m. Inspection of only the odd component of measured change does not allow determination of whether this feature is accretional or erosional. Inspection of the net shoreline change for this case reveals that this is an accretional feature on the updrift side of the inlet. Natural or man-made shoreline features can often introduce shoreline inhomogeneities that do not satisfy the assumptions of the methods used here. One possible future improvement to the numerical shoreline change model would be to account for inhomogeneities by allowing the diffusivity parameter, G, to vary along the domain.

Shoreline changes at inlets not well-suited to the assumptions implicit in the predictive methods presented here must often receive careful consideration for thorough understanding. Figure 10 shows the net shoreline change, and its even and odd components for Ponce de Leon Inlet, 1952–1973. This is a natural inlet that was stabilized by jetties in 1971, the northern jetty incorporating a weir in order to facilitate sand bypassing to the southern shore. The weir was closed in 1984 to reduce erosion on the northern side. The erosion on the updrift side (north; left in Figure 10) is evident in the figure, as is a very large accretional zone immediately downdrift of the inlet. This accretion is due primarily to the configuration of the downdrift jetty; as built, it formed a "pocket" that tended to trap material.

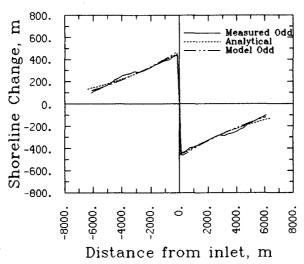


Figure 7: Measured odd component and predictions of shoreline change for St. Lucie Inlet, 1883–1967 (inlet constructed 1892). $H_b = 0.62 \text{ m}, \theta_b = 4.4 \text{ degrees}.$

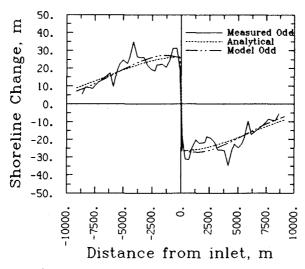


Figure 8: Measured odd component and predictions of shoreline change for Sebastian Inlet, 1946–1970 (inlet constructed 1924). $H_b = 0.75 \text{ m}$, $\theta_b = 0.8 \text{ degrees}$.

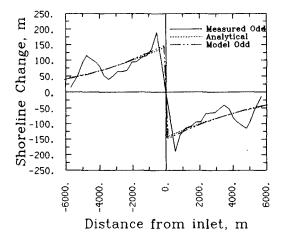


Figure 9: Measured odd component and predictions of shoreline change for Port Canaveral, 1951–1970 (inlet constructed 1951). $H_b = 1.07 \text{ m}$, $\theta_b = 1.4 \text{ degrees}$.

Another case of interest is that of a natural, unstabilized tidal inlet. Figure 11 provides the shoreline change components for Matanzas Inlet, 1923–1986. The position of the downdrift boundary of this inlet is partially restrained by a bridge abutment, and the downdrift shore is now heavily armored, but there are no jetty structures. Note that the even component of shoreline change indicates a slight gain of sediment within the domain, and the expected pattern of accretion updrift and erosion downdrift is present. Another future goal is to be able to accurately predict both bypassing rates and shoreline changes at an unstabilized tidal inlet.

Conclusions

Computation of shoreline changes at many of Florida's tidal inlets and decomposition of these signals into even and odd components reveals a fairly consistent updrift offset pattern, particularly at entrances that have been stabilized on both updrift and downdrift sides. Several inlets deviate from this trend, but the reasons are usually evident upon consideration of the history of the area.

The best-fit analytical solution developed matches the odd function well at several inlets showing a significant updrift offset, although it is not capable of predicting the small-scale features seen in the field. Reasonable values for the long-term wave climate are generated using the pre-bypassing analytical solution. Lack of reliable, long-term, directional wave data hinders complete assessment of results and remains a limitation to improved modelling efforts.

Refinement of the numerical model will be necessary to predict the small—scale features seen in the field. The wave transformation model could be improved by using higher—order wave theory, including wave—current interaction, providing a more sophisticated method for computation of tidal currents, and improving the wave breaking computations. Directional wave data would allow simulation of

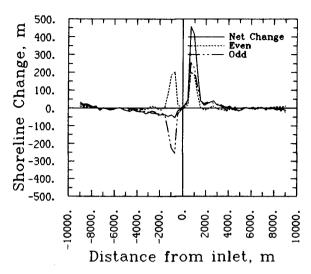


Figure 10: Net, even, and odd components of measured shoreline change for Ponce de Leon Inlet, 1952–1973.

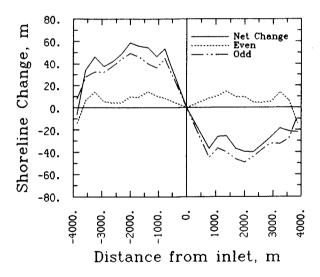


Figure 11: Net, even, and odd components of measured shoreline change for Matanzas Inlet, 1923–1986.

the longshore sediment transport reversals known to occur at many of Florida's inlets. The sediment transport model could be refined to account for the inhomogeneous nature of the shoreline in both the longshore and cross-shore directions.

The problems of interpretation and prediction of shoreline evolution adjacent to tidal inlets remains of both considerable interest and difficulty. Further refinement of the methods applied to date should lead to improved predictive ability.

Acknowledgement

Support provided by the Florida Sea Grant College Program of the National Oceanic and Atmospheric Administration under Project R/C-S-22 is hereby gratefully acknowledged.

References

BEREK, E.P., and DEAN, R.G. (1982).

Field Investigation of Longshore Transport Distribution. Proc. 18th Coastal Engineering Conference, ASCE, pp. 1620–1639.

DEAN, J.L., and POPE, J. (1987).

The Redington Shores Breakwater Project: Initial Response. Proc. Coastal Sediments '87, ASCE, pp. 1369–1384.

FOSTER, E.M., and SAVAGE, R.J. (1989)

Methods of Historical Shoreline Analysis. Proc. Coastal Zone '89, Sixth Symposium on Coastal and Ocean Management, Charleston, S.C. Vol. 5, pp. 4420-4433.

PELNARD-CONSIDÈRE, R. (1956).

Essai de Théorie de l'Evolution des Forms de Rivages en Plage de Sable et de Galets. 4th Journées de l'Hydraulique, les Energies de la Mer, Question III, Rapport No. 1, pp. 289–298.

PERLIN, M., and DEAN, R.G. (1985).

3-D Model of Bathymetric Response to Structures. Journal of Waterway, Port, Coastal, and Ocean Engineering, ASCE, Vol. 111, No. 2, pp. 153-170.

SAVAGE, R.J., and FOSTER, E.M. (1989)

Historical Shoreline Changes in Southeast Florida. Proc. Coastal Zone '89, Sixth Symposium on Coastal and Ocean Management, Charleston, S.C. Vol. 5, pp. 4406–4419.